

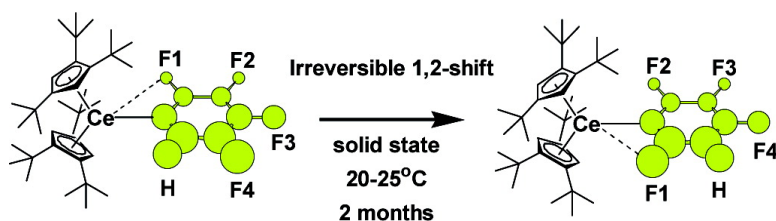
Article

Fluorine for Hydrogen Exchange in the Hydrofluorobenzene Derivatives CHF_x where $x = 2, 3, 4$ and 5 by Monomeric $[1,2,4\text{-}(\text{MeC})\text{CH}]_2\text{CeH}$: The Solid State Isomerization of $[1,2,4\text{-}(\text{MeC})\text{CH}]_2\text{Ce}(\text{2,3,4,5-CHF}_x)$ to $[1,2,4\text{-}(\text{MeC})\text{CH}]_2\text{Ce}(\text{2,3,4,6-CHF}_x)$

Evan L. Werkema, and Richard A. Andersen

J. Am. Chem. Soc., **2008**, 130 (22), 7153-7165 • DOI: 10.1021/ja800639f • Publication Date (Web): 09 May 2008

Downloaded from <http://pubs.acs.org> on February 8, 2009



More About This Article

Additional resources and features associated with this article are available within the HTML version:

- Supporting Information
- Links to the 3 articles that cite this article, as of the time of this article download
- Access to high resolution figures
- Links to articles and content related to this article
- Copyright permission to reproduce figures and/or text from this article

[View the Full Text HTML](#)

Fluorine for Hydrogen Exchange in the Hydrofluorobenzene Derivatives $C_6H_xF_{(6-x)}$, where $x = 2, 3, 4$ and 5 by Monomeric $[1,2,4-(Me_3C)_3C_5H_2]_2CeH$: The Solid State Isomerization of $[1,2,4-(Me_3C)_3C_5H_2]_2Ce(2,3,4,5-C_6HF_4)$ to $[1,2,4-(Me_3C)_3C_5H_2]_2Ce(2,3,4,6-C_6HF_4)$

Evan L. Werkema and Richard A. Andersen*

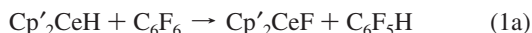
Chemistry Department and Chemical Sciences Division of Lawrence Berkeley National Laboratory, University of California, Berkeley, California 94720

Received January 30, 2008; E-mail: raandersen@lbl.gov

Abstract: The reaction between monomeric bis(1,2,4-tri-*tert*-butylcyclopentadienyl)cerium hydride, Cp'_2CeH , and several hydrofluorobenzene derivatives is described. The aryl derivatives that are the primary products, $Cp'_2Ce(C_6H_{5-x}F_x)$ where $x = 1, 2, 3, 4$, are thermally stable enough to be isolated in only two cases, since all of them decompose at different rates to Cp'_2CeF and a fluorobenzynes; the latter is trapped by either solvent when C_6D_6 is used or by a $Cp'H$ ring when C_6D_{12} is the solvent. The trapped products are identified by GC/MS analysis after hydrolysis. The aryl derivatives are generated cleanly by reaction of the metallocycle, $Cp'((Me_3C)_2C_5H_2C(Me_2)CH_2)Ce$, with a hydrofluorobenzene, and the resulting arylcerium products, in each case, are identified by their 1H and ^{19}F NMR spectra at 20 °C. The stereochemical principle that evolves from these studies is that the thermodynamic isomer is the one in which the CeC bond is flanked by two ortho-CF bonds. This orientation is suggested to arise from the negative charge that is localized on the ipso-carbon atom due to $C_o(\delta+)F_o(\delta-)$ polarization. The preferred regioisomer is determined by thermodynamic rather than kinetic effects; this is illustrated by the quantitative, irreversible solid-state conversion at 25 °C over two months of $Cp'_2Ce(2,3,4,5-C_6HF_4)$ to $Cp'_2Ce(2,3,4,6-C_6HF_4)$, an isomerization that involves a CeC(ipso) for C(ortho)F site exchange.

1. Introduction

The fluoride for hydrogen-exchange reactions that resulted when C_6F_6 or C_6HF_5 was added to monomeric $[1,2,4-(Me_3C)_3C_5H_2]_2CeH$, abbreviated as Cp'_2CeH , have been described recently.¹ The initial products of the reaction of C_6F_6 and Cp'_2CeH were $Cp'_2CeC_6F_5$, Cp'_2CeF , and H_2 ; the pentafluoroaryl derivative decomposed to the fluoride and tetrafluorobenzynes, which was trapped by either C_6D_6 (solvent), or the Cp' -ring of a metallocene. Hydrogen was suggested to be formed in two sequential reactions illustrated in eqs 1a and 1b. Thus, the net F-/H-exchange reaction was composed of individual intermolecular CF and CH activation steps.



DFT calculations on the reaction between $(C_5H_5)_2LaH$, used as a model for the experimental reaction, and either C_6F_6 or C_6F_5H showed that the CH activation barrier, eq 1b, is substantially lower than the CF activation barrier, eq 1a, but the elimination of C_6F_4 from $Cp'_2CeC_6F_5$ proceeded with a higher barrier. The experimental studies required that the net CF and CH activation barriers were comparable since the products derived from each process were observed, which was

inconsistent with the calculated potential energy surfaces. The postulate that CH activation barriers are lower, higher, or comparable to CF barriers can be tested by experimental studies of the reaction between Cp'_2CeH and judiciously chosen isomeric hydrofluorobenzenes. The results of these experimental studies are the subject of this paper.

2. Results

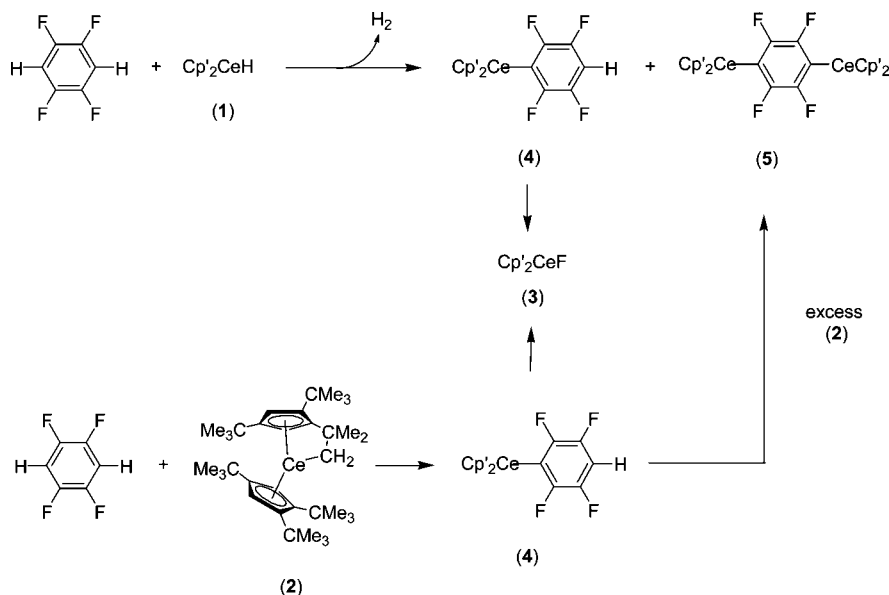
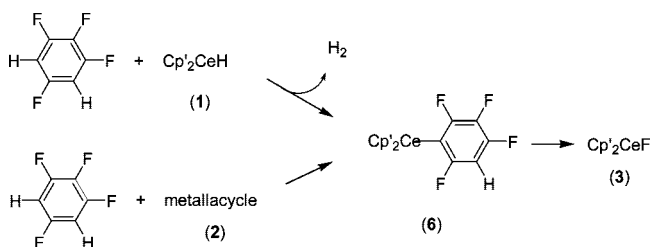
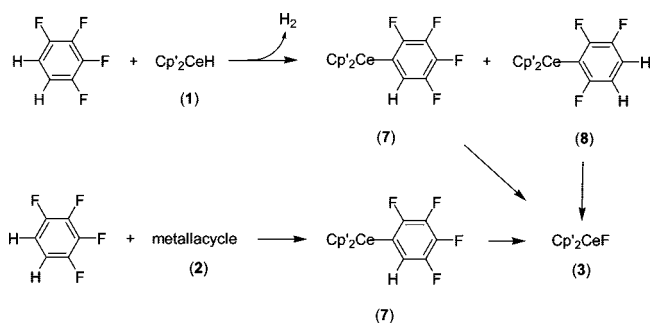
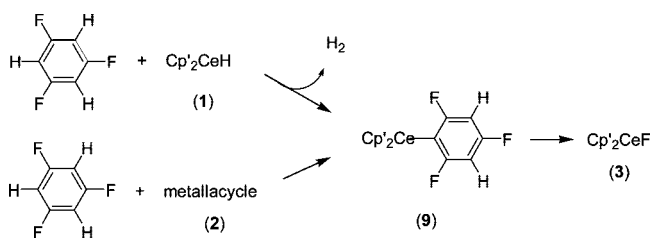
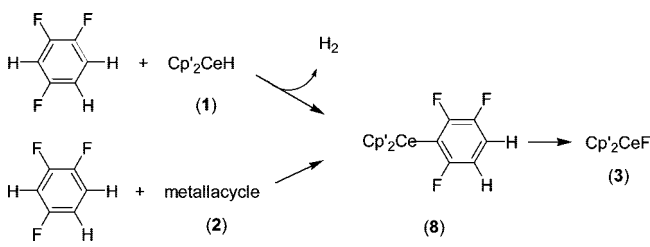
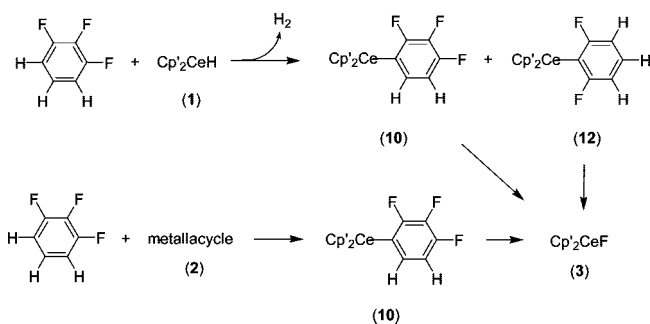
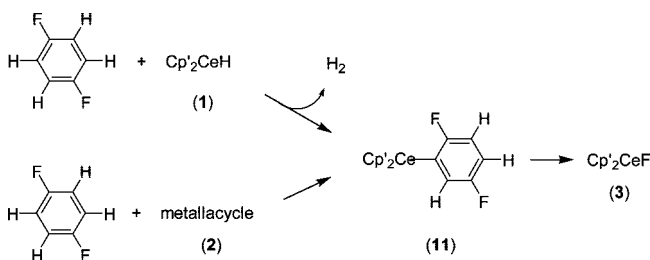
2.1. Strategy. In general, the products formed in the reaction of Cp'_2CeH , **1**, and the hydrofluorobenzene derivatives described below are not isolated as crystalline materials because of their thermal instability, as mentioned in earlier papers.^{1,2} The changes that occur in the 1H and ^{19}F NMR spectra however are readily observed, and these changes are monitored as a function of time. Even when the fluoroaryl derivatives are isolated by crystallization, they do not give satisfactory combustion analysis, as is well-known for fluorocarbon compounds.³ The compounds do not yield molecular ions in their mass spectra; instead they give fragmentation ions and do not sublime nor melt without decomposition.

The identity of the products is ascertained by comparison of the 1H and ^{19}F NMR spectral features obtained by reaction of

(1) Maron, L.; Werkema, E. L.; Perrin, L.; Eisenstein, O.; Andersen, R. A. *J. Am. Chem. Soc.* **2005**, *127*, 279–292.

(2) Werkema, E. L.; Messines, E.; Perrin, L.; Maron, L.; Eisenstein, O.; Andersen, R. A. *J. Am. Chem. Soc.* **2005**, *127*, 7781–7795.

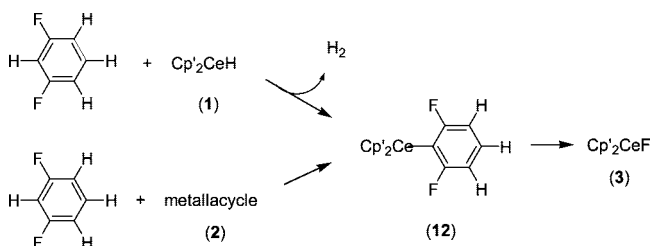
(3) Banks, R. E. *Fluorocarbons and Their Derivatives*, 2nd ed.; MacDonald and Company: London, 1970; p 17.

Scheme 1. Reactions of 1,2,4,5-Tetrafluorobenzene**Scheme 2.** Reactions of 1,2,3,5-Tetrafluorobenzene**Scheme 3.** Reactions of 1,2,3,4-Tetrafluorobenzene**Scheme 4.** Reactions of 1,3,5-Trifluorobenzene**Scheme 5.** Reactions of 1,2,4-Trifluorobenzene**Scheme 6.** Reactions of 1,2,3-Trifluorobenzene**Scheme 7.** Reactions of 1,4-Difluorobenzene

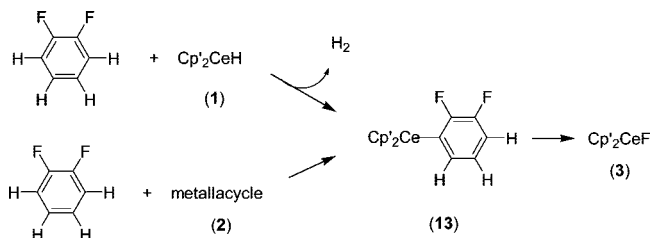
the metallacycle $\text{Cp}'((\text{Me}_3\text{C})_2\text{C}_5\text{H}_2\text{C}(\text{Me}_2)\text{CH}_2)\text{Ce}$, **2**, Schemes 1–9, and a hydrofluorobenzene, which only yields the fluoroaryl derivatives resulting from insertion of a CH bond into the CeC bond of the metallacycle. When isomeric fluoroaryl derivatives are possible, judicious choice of the hydrofluorobenzene yields spectra that match those obtained in the reaction of $\text{Cp}'_2\text{CeH}$. In this manner, the identity and stereochemistry of the fluoroaryl

derivative is delineated. The ^1H and ^{19}F NMR spectra listed in Table 1 are acquired in this manner. Hydrolysis of the reaction mixture (H_2O) and examination of the hydrolysate by ^{19}F NMR spectroscopy identifies and quantifies the hydrofluorobenzene or benzenes formed. In general, this protocol shows that the reactions are clean when the reaction times are short. The NMR

Scheme 8. Reactions of 1,3-Difluorobenzene



Scheme 9. Reactions of 1,2-Difluorobenzene



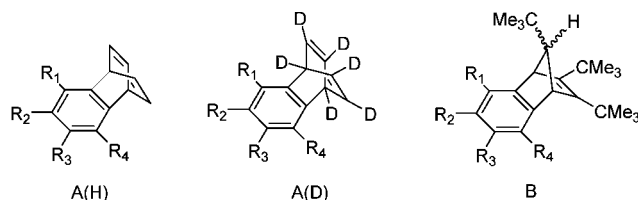
spectra of the mixtures in either C_6D_6 or C_6D_{12} are monitored over time, at 20 or 60 °C, until the resonances due to $Cp'2CeH$ disappear and those of $Cp'2CeF$ are the only paramagnetic resonances remaining. The organic products are identified (after hydrolysis (H_2O)) by GC/MS analysis as derived from trapping of the fluoroaryne by either C_6H_6 [A(H)], C_6D_6 [A(D)], or $Cp'H$ (B) when C_6H_6 , C_6D_6 , or C_6D_{12} is the solvent, respectively, Chart 1. Once the library of 1H and ^{19}F NMR spectra are acquired, Table 1, the products of the reaction between $Cp'2CeH$ and $C_6H_xF_{(6-x)}$ ($x = 5,4,3,2$) are readily identified. The first formed product, called the primary product, is readily identified, as are the subsequent or secondary products. Only two fluoroaryl derivatives are isolated as pure solids, and both are characterized by single crystal X-ray crystallography.

2.2. Solution Studies. 2.2.1. Reaction of 1 and 2 with Isomeric Tetrafluorobenzenes. 2.2.1.1. 1,2,4,5- $C_6H_2F_4$, Scheme 1. Addition of an excess of 1,2,4,5-tetrafluorobenzene to a purple solution of $Cp'2CeH$, **1**, in C_6D_6 at 20 °C in an NMR tube results in an immediate color change to orange and gas evolution (H_2). Examination of the solution by 1H NMR spectroscopy within 20 min shows the presence of two new sets of paramagnetic resonances, each of which appear in a 2:1 area ratio due to the Me_3C groups, in a 1.5:1 area ratio along with a resonance due to H_2 and tiny resonances due to $Cp'2CeF$, **3**; resonances due to $Cp'2CeH$ are absent. The identity of one of the two new sets of resonances is established by adding an excess of 1,2,4,5- $C_6H_2F_4$ to the metallacycle, **2**, in C_6D_{12} in an NMR tube at 20 °C. The 1H NMR spectrum of this mixture identifies this set of resonances as due to **4**, Table 1. Evaporating the contents of the NMR tube to dryness (in order to remove excess 1,2,4,5- $C_6H_2F_4$), redissolving the residue in C_6D_{12} , and adding a small quantity of **2** results in appearance of the resonances in the 1H NMR spectrum due to **5** at the expense of those due to **4**. Addition of more **2** increases the resonances due to **5**, again at the expense of those due to **4**. These experiments are sufficient to identify **4** and **5** as the fluoroaryl derivatives derived by insertion of the CH bond into the CeC bond of **2**, Scheme 1. The 1H NMR spectrum of **4** also contains a triplet resonance due to a single proton ($J = 7$ Hz) that is assigned to the para-H in **4**. The ^{19}F NMR spectrum of **4** contains two broad resonances assigned to the ortho-F and the meta-F groups, Table 1.

Table 1. 1H and ^{19}F NMR Chemical Shifts^a

compd	1H NMR				^{19}F NMR			
	Cp'-ring		$C_6H_xF_x$		o-F		m-F	
	CMes	CMes	o-H	m-H	p-H	p-F	m-F	p-F
$Cp'2CeH$, ^a 1 , C_6D_6	-3.44(45)	-3.44(45)	-	-	-	-	-	-
$Cp'2CeF$, ^a 3 , C_6D_6	-2.50(10)	-2.50(10)	-	-	-	-	-	-157.6 t $J = 18$
$Cp'2CeC_6F_5$ ^a	-1.77(190)	-1.77(190)	-	-	-	-	-	-141(30)
$Cp'2Ce(2,3,5,6-C_6HF_4)$, 4	-1.84(130)	-1.84(130)	-	-	3.70 t $J = 7$	-	-	-139 dd $J = 18,7$
$Cp'2Ce(2,3,4,6-C_6HF_4)$, 6	-1.44(100)	-2.09(90)	-	-	-	-	-	-161.6 dd $J = 18$
$Cp'2Ce(2,3,4,5-C_6HF_4)$, 7	-1.90(120)	-1.90(120)	not obsd	-	-	-	-	-161.8 d $J = 18$ -137.0 d $J = 18$
$Cp'2Ce(2,3,6-C_6H_2F_3)$, 8	-1.46(70)	-2.17(60)	-	-	-	-	-	-142(30)
$Cp'2Ce(2,4,6-C_6H_2F_3)$, 9	-1.73(50)	-1.73(50)	-	-	0.41 t $J = 8$	-	-	-
$Cp'2Ce(2,3,4-C_6H_2F_3)$, 10	-1.83(50)	-1.83(50)	-	-	-	-	-	-115 t $J = 16$
$Cp'2Ce(2,5-C_6H_3F_2)$, 11	-1.93(40)	-1.93(40)	not obsd	-	4.75 dd $J = 8,8$	-	-	-137 dd $J = 18,6$
$Cp'2Ce(2,6-C_6H_3F_2)$, 12	-1.77(40)	-1.77(40)	not obsd	-	0.42(10)	-	-	-
$Cp'2Ce(2,3-C_6H_3F_2)$, 13	-1.21(50)	-1.21(50)	-	-	2.50 d $J = 8$	-	-	-
$Cp'2Ce(2-C_6H_4F)$, 14	<i>b</i>	<i>b</i>	<i>b</i>	<i>b</i>	<i>b</i>	<i>b</i>	<i>b</i>	-

^a C_6D_{12} unless otherwise stated at 20 °C. ^{19}F NMR chemical shifts are quoted relative to $CFCl_3$ ($\delta = 0$). Negative values are due to high field or low frequency of $CFCl_3$. The line width in Hz, $\nu_{1/2}$, is listed in parentheses below the chemical shift. The coupling constants are listed after the chemical shift along with the multiplicity. The chemical shifts of the 1,2,4-tri-*tert*-butylcyclopentadienyl ring methylenes are not listed. ^b The compound decomposes to $Cp'2CeF$ rapidly, and the low-intensity 1H and ^{19}F resonances cannot be assigned with confidence.

Chart 1. Cycloaddition Products of Fluorobenzyne with C₆H₆, C₆D₆, or Cp'H

	R ₁	R ₂	R ₃	R ₄
Product identity				
A(H)-1	F	F	H	F
A(D)-1	F	F	H	F
B-1	F	F	H	F
B-2	F	F	F	H
B-3	F	H	H	F
B-4	H	H	F	F
B-5	H	H	H	F
B-6	H	H	H	H

Variable-temperature NMR spectra of **4** and several other fluoroaryl derivatives are described later in this article.

The reaction between **1** and 1,2,4,5-C₆H₂F₄ in C₆D₁₂ at 20 °C after 20 min yields resonances due to **4** and **5** in comparable amounts and H₂, as when C₆D₆ is the solvent. These primary products are derived from exchange between CeH and CH groups and therefore by CH activation of the hydrofluorobenzene. The resonances due to **4** and **5** diminish, while those due to **3** appear over time. After one day (20 °C), the resonances due to **5** are gone, and the resonances due to **4** and **3** are present in a ratio of 18:1. After 11 days, the ratio is 1:4, and paramagnetic resonances due to **X** (see later) begin to appear as do several resonances in the diamagnetic region ($\delta = 0-2$). After 17 days, the resonances due to **X** increase in intensity, as do the resonances in the diamagnetic region, at the expense of those due to **4**. Heating to 60 °C for one day yields a ¹H NMR spectrum that contains paramagnetic resonances due only to **3** and **X** in a 6:1 ratio (assuming that the cyclopentadienyl ring in **X** contains three CMe₃ groups). These two sets of resonances account for about 30% of the Cp' groups originally present in Cp'₂CeH, and therefore the "diamagnetic resonances" have appreciable intensity.

Repeating the reaction of **1** with an excess of 1,2,4,5-C₆H₂F₄ in C₆H₆ followed by heating to 60 °C for one day, evaporation of the solvent, and dissolution of the residue in C₆D₆ shows resonances in the ¹H NMR spectrum due to **3** and **X** in a 7:1 ratio and resonances in the ¹H and ¹⁹F NMR spectra due to A(H)-1, Chart 1.⁴ Hydrolysis (H₂O) and analysis by GC/MS shows a single component with *m/z* of 208 due to A(H)-1, Chart 1. When the solvent is C₆D₆, the GC/MS shows a single component with *m/z* of 214 due to A(D)-1, Chart 1, and the ¹⁹F NMR spectrum contains resonances due to A(D)-1.

Repeating the reaction between **1** and 1,2,4,5-C₆H₂F₄ in C₆D₁₂ at 20 °C yields ¹H and ¹⁹F NMR spectra that are qualitatively similar to those in C₆D₆ or C₆H₆. However, at the end of the reaction the ratio of **3** to **X** is about 2:1; more **X** is formed

when C₆D₁₂ is the solvent. Evaporation of C₆D₁₂ followed by hydrolysis and analysis by GC/MS showed three major components (along with Cp'H and C₆D₁₂), one with an *m/z* value of 364 due to B-1 and the other two with *m/z* values of 307 (M - CMe₃)⁺ due to the two other possible isomers of B-1, Chart 1, which arise from the [2 + 4] cycloaddition reaction between 3,4,6-trifluorobenzyne and Cp'H. In this reaction, C₆D₆ or C₆H₆ is not available to trap the benzyne, and the Cp'-ring is the trap. A larger amount of **X** forms when C₆D₁₂ is the solvent relative to **3**, suggesting that **X** is a cerium containing species that contains one substituted cyclopentadienyl ring, but its identity is a mystery. It is noteworthy that **X** forms even when C₆D₆ is the solvent, suggesting that the substituted cyclopentadienyl ligands can trap the fluorobenzyne even when C₆D₆ is present in large excess.

2.2.1.2. 1,2,3,5-C₆H₂F₄, Scheme 2. The reaction between 1,2,3,5-tetrafluorobenzene and Cp'₂CeH at 20 °C in C₆D₁₂ in an NMR tube is qualitatively similar to that observed with 1,2,4,5-tetrafluorobenzene. New paramagnetic resonances appear in the ¹H NMR spectrum due to the cyclopentadienyl Me₃C groups in an area ratio of 1:1:1. In addition, resonances due to H₂ and **3** appear; the ratio of the new resonances to those of **3** is about 4:1. The same three Me₃C group resonances appear in the ¹H NMR spectrum when an excess of 1,2,3,5-C₆H₂F₄ is added to the metallacycle **2** in C₆D₁₂, Scheme 2. The ¹H NMR spectrum also contains a triplet resonance, *J* = 7 Hz, due to a single proton, and the ¹⁹F NMR spectrum shows four equal area resonances, two of which are broad and two of which are narrow enough for the coupling pattern to be visible, viz., a doublet (*J* = 15 Hz) and a doublet of doublets with *J* = 18 and 7 Hz, Table 1. These data are sufficient to identify the product as **6**, Scheme 2, the product resulting from intermolecular CH activation. The appearance of three chemically inequivalent Me₃C resonances is expected for **6** with averaged C_s symmetry as is observed at 20 °C, Table 1; the variable-temperature NMR spectra are described below.

When **6** is generated in the reaction of **2** with 1,2,3,5-C₆H₂F₄, it is stable at 20 °C for days in C₆D₁₂. When heated to 60 °C

(4) Harrison, R.; Heaney, H. *J. Chem. Soc. C* **1968**, 889–892.

for two days, all of the resonances due to **6** disappear, and resonances due to **3** and **X** appear in approximately equal amounts as well as a number of other resonances in the diamagnetic region. Hydrolysis and analysis of the hydrolysate by GC/MS show six components (in addition to Cp'H), two with m/z 364 and four with m/z 307 ($M - CMe_3$)⁺ in an approximate ratio of 3:11:1:1:6:7, respectively, which are attributed to the six isomers resulting from the [2 + 4] cycloaddition of 3,4,6- and 3,4,5-trifluorobenzynes with Cp'H, viz., B-1 and B-2, respectively. The retention times and isotopic patterns for the six components matched those obtained from hydrolysis of the thermal decomposition of **4** and **7** (see later).

2.2.1.3. 1,2,3,4-C₆H₂F₄, Scheme 3. Addition of 1,2,3,4-tetrafluorobenzene to a solution of Cp'₂CeH in C₆D₁₂ in an NMR tube at 20 °C results in an orange solution that contains two new sets of paramagnetic Me₃C resonances in a net area ratio of 2:1; the resonances of the former display a 1:1:1 pattern for the Me₃C groups while those of the latter appear in a 2:1 ratio. The spectrum also contains resonances due to **3** and H₂. The new resonances are identified in the following manner. Addition of 1,2,3,4-C₆H₂F₄ to a solution of the metallacycle **2** in C₆D₁₂ generates a ¹H NMR spectrum in which the Me₃C resonances appear in a 2:1 ratio with the same chemical shifts as those mentioned above. The ¹⁹F NMR spectrum contains three equal area resonances, two of which appear as doublets ($J = 18$ Hz) and one as a triplet ($J = 18$ Hz), Table 1. This pattern is consistent with that expected for **7**, Scheme 3, assuming that the resonance for the ortho-F is broadened into the baseline. The other resonances are identified as those due to **8**, Scheme 3, since addition of 1,2,4-trifluorobenzene to **2** generates a ¹H NMR spectrum whose chemical shifts are identical to the 1:1:1 pattern of resonances with relative area 2, Scheme 5.

The aryl derivative **7** results from a net CeH for CH exchange, while **8** is derived from a net CeH for CF exchange. Apparently, the major primary product of the reaction of Cp'₂CeH and 1,2,3,4-C₆H₂F₄ is not derived from CH activation but from a CF activation process. This observation contradicts the postulate that CH activation proceeds with a lower barrier than CF activation, a postulate derived from DFT calculations on the reaction of Cp₂LaH and C₆HF₅. This apparent contradiction caused us to examine more carefully the NMR spectra obtained in the reaction of **1** and C₆HF₅, reported earlier.¹ Re-examination shows that Cp'₂CeC₆F₅ is indeed the major product as described, but small but not insignificant resonances due to **4**, Scheme 1, are also observed in the ¹H and ¹⁹F NMR spectra at short reaction times. Thus, our postulate that net CH activation always proceeds with a lower activation barrier than CF activation does is inconsistent with the experimental observations and needs to be modified.

Over time, the resonances due to **7** and **8** disappear (at different rates), and the resonances due to **3**, **X**, and those in the diamagnetic region increase in intensity. Heating at 60 °C for one day results in only those resonances due to **3**, **X**, and the "diamagnetic ones." Hydrolysis of the thermal decomposition products of **7**, prepared from **2**, and analysis of the organic products by GC/MS show three primary components along with Cp'H, one with m/z of 364 and two with m/z of 307 ($M - CMe_3$)⁺ in a 4:1:6 ratio, respectively, due to isomers of B-2, Chart 1; several isomers of the structure represented by B can form, depending upon which Cp'-ring carbon atoms participate in the [4 + 2] cycloaddition reaction.

When the thermal decomposition of **7**, prepared from **2**, is monitored closely at 20 °C, small resonances due to **6** appear

and then disappear over the course of a day as those of **3** appear. This surprising observation is described later in more detail.

2.2.2. Reaction of 1 and 2 with Isomeric Trifluorobenzenes. 2.2.2.1. 1,3,5-C₆H₃F₃, Scheme 4. Addition of 1,3,5-trifluorobenzene to Cp'₂CeH in C₆D₁₂ at 20 °C and monitoring by ¹H NMR spectroscopy results in the appearance of two new Me₃C resonances in a 2:1 ratio and a doublet ($J = 9$ Hz) due to two hydrogens. These are the resonances expected for aryl derivative **9**, Scheme 4. Reaction of 1,3,5-C₆H₃F₃ with metallacycle **2** generates only resonances due to **9** in the ¹H NMR spectrum. The ¹⁹F NMR spectrum consists of two resonances in a 2:1 ratio; the former is very broad, while the latter is a triplet ($J = 10$ Hz), Table 1. Over time, the resonances due to **9** are replaced by those due to **3**, **X**, and diamagnetic ones.

2.2.2.2. 1,2,4-C₆H₃F₃, Scheme 5. Addition of 1,2,4-trifluorobenzene to a C₆D₁₂ solution of Cp'₂CeH in an NMR tube at 20 °C yields a new set of Me₃C resonances in the ¹H NMR spectrum in a relative ratio of 1:1:1 and two resonances due to one hydrogen each that are a doublet and an apparent triplet, $J = 8$ Hz in each case. Three possible isomers can result from CeH for CH exchange, but the ¹H NMR spectrum is consistent with the one illustrated as **8** in Scheme 5. The structural assignment is supported by generating **8** from the metallacycle, **2**, and 1,2,4-C₆H₃F₃ and observing the ¹H and ¹⁹F NMR spectra, Table 1. The compound **8** has C_s symmetry, assuming that the Cp' rings are free to rotate, and therefore the CMe₃ groups on a given cyclopentadienyl ring are chemically inequivalent and will appear as a 1:1:1 pattern, as observed. Heating **8** to 60 °C for 12 h results in disappearance of the resonances due to **8** and formation of those due to **3**, **X**, and diamagnetic resonances. Hydrolysis and analysis of the hydrolysate by GC/MS shows five components in the mixture in an approximate ratio of 3:3:3:2:2, four of which exhibit m/z of 346 and one with m/z of 289 ($M - CMe_3$)⁺ due to the isomers B-3 and B-4.

2.2.2.3. 1,2,3-C₆H₃F₃, Scheme 6. In contrast to the reaction of the two isomers of C₆H₃F₃ just described, which give single regioisomers, **8** and **9**, 1,2,3-trifluorobenzene gives two aryl derivatives. Examination of the solution formed upon addition of 1,2,3-trifluorobenzene to Cp'₂CeH in C₆D₁₂ in an NMR tube at 20 °C by ¹H NMR spectroscopy shows a pair of overlapping Me₃C resonances in a 2:1 area ratio, along with resonances due to **1**, **3**, and H₂. After 3 h, the minor set of Me₃C resonances disappears, and those due to the major product consist of Me₃C resonances in a 2:1 area ratio, a triplet ($J = 8$ Hz) and a doublet ($J = 8$ Hz) due to one and two hydrogens each, respectively, Table 1; the ¹⁹F NMR spectrum consists of a broad single resonance. The ¹H NMR spectrum of the major product is identical to that of **12**, derived by addition of 1,3-difluorobenzene to the metallacycle **2**, Scheme 8, see below. Thus, the major product is derived from CF activation. The minor isomer is the CH activation product **10**, which is prepared cleanly from the metallacycle **2**, Scheme 6. As in the reaction of 1,2,3,4-tetrafluorobenzene, the primary product is that derived by CeH for CF exchange. After one day at 20 °C the ratio of **3** to **10** is 4:1 and after an additional day at 60 °C, only resonances due to **3**, **X**, and diamagnetic resonances are present in the ¹H NMR spectrum. Thus, the major product formed in this reaction is derived from CeH for CF exchange, as in the reaction between **1** and 1,2,3,4-tetrafluorobenzene.

2.2.3. Reaction of 1 and 2 with Isomeric Difluorobenzenes and Fluorobenzene. 2.2.3.1. 1,4-C₆H₄F₂, Scheme 7. Addition of 1,4-difluorobenzene to Cp'₂CeH or the metallacycle **2** generates identical ¹H NMR spectra which, along with their

^{19}F NMR spectra, are listed in Table 1. The spectra are in accord with those expected for **11**, Scheme 7. With time, the resonances disappear and are replaced by those due to **3**, **X**, and diamagnetic ones.

2.2.3.2. 1,3- $\text{C}_6\text{H}_4\text{F}_2$, Scheme 8. This fluorobenzene derivative reacts with either $\text{Cp}'_2\text{CeH}$ or the metallacycle **2** to give identical ^1H and ^{19}F NMR spectra, Table 1, which are consistent with an aryl derivative with structure **12**, Scheme 8. With time, resonances due to **12** disappear, and those due to **3**, **X**, and diamagnetic resonances appear.

2.2.3.3. 1,2- $\text{C}_6\text{H}_4\text{F}_2$, Scheme 9. Addition of 1,2-difluorobenzene to $\text{Cp}'_2\text{CeH}$ at 20 °C in C_6D_{12} yields a red-purple solution, which turns orange over 30 min. After 5 min, the ^1H NMR spectrum contains Me_3C resonances in a 2:1 area ratio and three resonances due to one hydrogen each that are a singlet, a doublet ($J = 8$ Hz), and a triplet ($J = 8$ Hz), Table 1. These resonances are consistent with those expected for **13**, Scheme 9. After 30 min at 20 °C, the ratio of **1**, **3**, and **13** is 2:4.5:1, and after one day at 20 °C, the only paramagnetic resonances visible are those due to **3** and diamagnetic resonances which are attributed to B-5. Unfortunately, the aryl derivatives formed by the reaction of 1,2-difluorobenzene with the metallacycle, **2**, are not stable, and the amount of **13** that forms is not sufficient to obtain a satisfactory ^{19}F NMR spectrum.

2.2.3.4. $\text{C}_6\text{H}_5\text{F}$. The reaction of fluorobenzene with $\text{Cp}'_2\text{CeH}$ is related to that of the difluorobenzenes since it is slow, and the lifetime of the fluoroaryl product, relative to decomposition to **3**, is insufficient to acquire satisfactory ^1H or ^{19}F NMR spectra. A small amount of **3** is generated initially, along with diamagnetic resonances of considerable intensity. Hydrolysis and analysis by GC/MS yields one component with m/z of 310, due to B-6 (Chart 1).

In summary, these four fluorobenzenes give cerium fluoroaryl derivatives resulting from CeH for CH exchange.

2.2.4. NMR Spectroscopy. The solution ^1H and ^{19}F NMR spectra in either C_6D_{12} or C_6D_6 at 20 °C of the metallocene-cerium fluoroaryls generated and/or isolated that are described in this article are listed in Table 1. The Me_3C resonances are readily assigned on the basis of their relative area ratios; their chemical shifts lie in a narrow range between $\delta = -1.5$ to -2.2 ppm and $\delta = -9$ to -10 ppm. The Me_3C resonances are rather broad, and the resonances due to the cyclopentadienyl ring methylenes are often very broad or not visible. The ^{19}F NMR spectra are assigned on the basis of their relative area ratios and spin–spin coupling patterns. The H–F spin–spin coupling is also observed in the ^1H NMR spectra of those fluoroaryl derivatives that contain hydrogens. In general, the resonances due to hydrogen or fluorine atoms in the ortho sites are either very broad or unobserved, whereas those in the meta or para sites are always observed and narrow enough that the multiplicities due to spin–spin coupling are visible. The ^{19}F NMR chemical shifts of the meta-F and para-F resonances generally lie in the range of $\delta = -140$ to -165 ppm. The ortho-F resonances are further upfield in the range of $\delta = -210$ to -285 ; when the ortho-F sites are inequivalent, the resonances are separated by about 90 ppm as in **6** and **8**.

The Me_3C resonances of the 1,2,4-(Me_3C) $_3\text{C}_5\text{H}_2$ ring on the metallocene derivatives at 20 °C appear as an A_2X or an AMX pattern, Table 1. Assuming that the Cp' -rings are free to rotate or oscillate about their C_5 axes in the complexes in which the fluorobenzene ring is symmetrically substituted, the metallocene will have averaged C_{2v} symmetry, and the Me_3C resonances will appear in a 2:1 area ratio, as found in **4**, **9**, and **12**. When

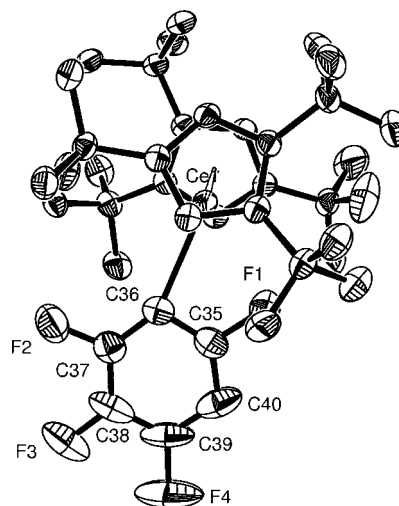


Figure 1. ORTEP diagram of $\text{Cp}'_2\text{Ce}(2,3,4,6\text{-C}_6\text{HF}_4)$, **6**, 50% thermal ellipsoids. The heavy atoms are refined anisotropically. Hydrogen atoms (not shown) are placed in calculated positions and not refined. The fluorine atom F(3) is disordered over two sites, C(37) and C(40), and the disorder was modeled as F(3) on C(37) 75% and F(5) (not shown) on C(40) 25%. The asymmetric unit contains one-half of a molecule of pentane, which is not shown.

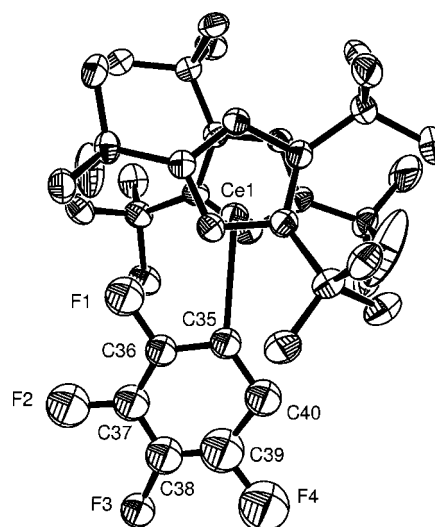


Figure 2. Solid state structure of $\text{Cp}'_2\text{Ce}(2,3,4,5\text{-C}_6\text{HF}_4)$, **7**, 50% thermal ellipsoids. The 50/50 disorder of the fluoroaryl ring is simplified to show one orientation; the Cp' -ring carbons and Ce atom are ordered and refined anisotropically, but the C_6HF_4 ring carbon and fluorine atoms are refined isotropically. The solid contains one-half of a molecule of disordered pentane, which is not shown.

the fluoroaryl ring is asymmetrically substituted, the C_2 axis and a vertical plane of symmetry are absent, the molecule has averaged C_s symmetry, and the Me_3C group resonances will appear in a 1:1:1 ratio, as in **6** and **8**.

The NMR spectra are averaged spectra, assuming that the solid state structures of these metallocene derivatives are similar to those of $\text{Cp}'_2\text{CeC}_6\text{F}_5$ ¹ and the two structures reported in this article, Figures 1 and 2, which are described in more detail below, in which there is one short $\text{Ce}\cdots\text{ortho-F}$ contact and the molecules have no symmetry. A physical process that involves the synchronous breaking and making of $\text{Ce}\cdots\text{ortho-F}$ bonds is sufficient to account for the observed ^1H NMR spectra at 20 °C. It is important to note that this fluxional motion will not result in the two ortho-F substituents exchanging sites; the

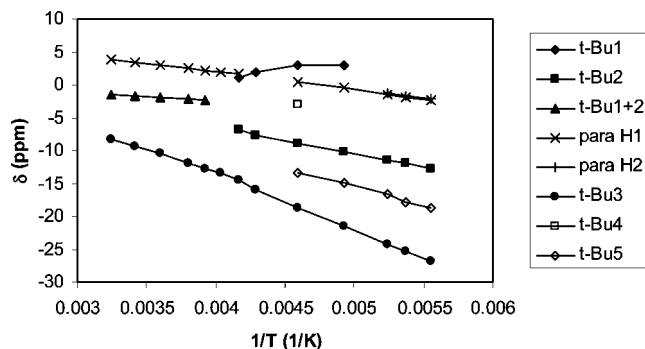


Figure 3. δ vs $1/T$ plot of the ^1H NMR resonances of $\text{Cp}'_2\text{Ce}(2,3,5,6\text{-C}_6\text{HF}_4)$, **4**, in C_7D_{14} , T in Kelvin.

physical process of rotation is required for ortho-F/ortho-F site exchange. For example, the ^{19}F NMR spectrum of **9** at 20°C has two resonances, which shows that the chemically inequivalent ortho-F and meta-H groups are averaged and, since the Me_3C groups appear in a 2:1 area ratio, **9** has averaged C_{2v} symmetry, and oscillation of the 2,4,6- $\text{C}_6\text{H}_2\text{F}_3$ group about the Ce–C(ipso) axis is a physical process that accounts for the averaged spectra. However, the observation that the Me_3C groups in **7**, **10**, **11**, and **13**, in which the ortho sites contain a fluorine and a hydrogen substituent, show an A_2X pattern at 20°C requires that additional fluxions must be occurring. Rotation about the Ce–C(ipso) bond by $\pi/2$ to generate a time-averaged mirror plane is one such physical process; this motion can occur with the Ce \cdots ortho-F interaction “in place” or with the Ce \cdots ortho-F interaction broken. In either case, rotation by $\pi/2$ is sufficient to render the adjacent Me_3C groups on the cyclopentadienyl ring equivalent in **7**, **10**, **11**, and **13**.

The variable-temperature ^1H and ^{19}F NMR spectra in C_{14}D_8 of several of the compounds listed in Table 1 were studied in order to explore the ring dynamics in more detail. A limitation is that the fluoroaryl derivatives decompose at varying rates at temperatures above 20°C , and only the low temperature behavior is studied. As the temperature is lowered to -50°C , the Me_3C resonance of area 2 decoalesces into two equal area resonances for **4**, **7**, **9**, **10**, and $\text{Cp}'_2\text{CeC}_6\text{F}_5$,¹ consistent with a molecule of C_s symmetry. The activation barriers $\Delta G^\ddagger_{(\text{TC})}$ for this process are approximately 10 kcal mol^{-1} in each case. As the temperature is lowered from -50 to -80°C , at least one and often all three Me_3C resonances grow another resonance, the total intensity of which is about one-third that of the original resonance. This behavior is clearly seen in the low-temperature ^1H NMR spectra of **4** and **9**. The unequal population shows that the line-shape is not due to an equal population decoalescence phenomenon but is, perhaps, most likely due to the presence of another rotamer in which the orientation of the substituted cyclopentadienyl rings in the metallocene are different but the averaged symmetry is still C_s . The ^1H NMR spectrum of **4** is consistent with this interpretation since the para-H resonance, represented as δ vs T^{-1} plots in Figures 3 and 4, is a single, sharp resonance down to about -70°C , when another resonance whose intensity at -80°C is about 10% of the original resonance, appears as shown in Figure 3.

The temperature dependence of the ^{19}F NMR spectra of several of the compounds listed in Table 1 also show common features. The most shielded and very broad resonance is attributed to the ortho-F resonance due to its proximity to the paramagnetic center, and this resonance is highly temperature dependent. When the ortho-F sites are inequivalent, as in **6** or

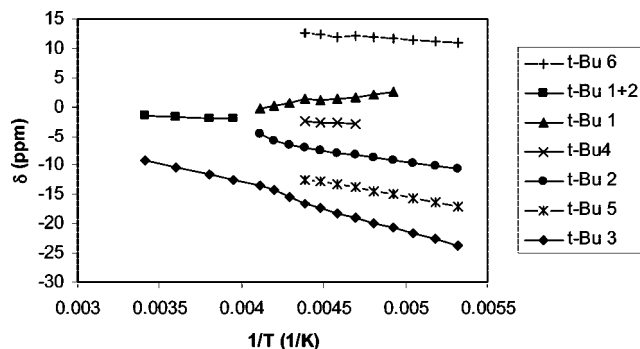


Figure 4. δ vs $1/T$ plot of the ^1H NMR resonances of $\text{Cp}'_2\text{Ce}'(2,4,6\text{-C}_6\text{H}_2\text{F}_3)$, **9**, in C_7D_{14} , T in Kelvin.

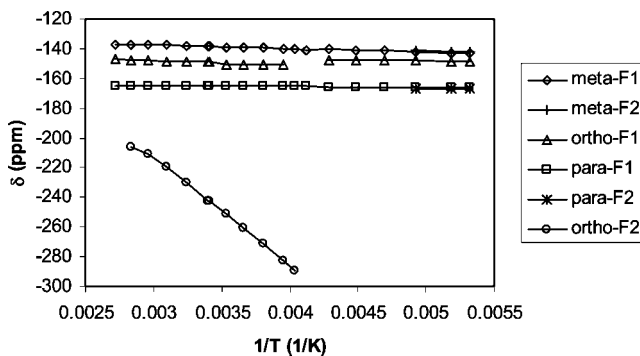


Figure 5. δ vs $1/T$ plot of the ^{19}F NMR resonances of $\text{Cp}'_2\text{Ce}'(2,3,4,6\text{-C}_6\text{HF}_4)$, **6**, in C_7D_{14} , T in Kelvin.

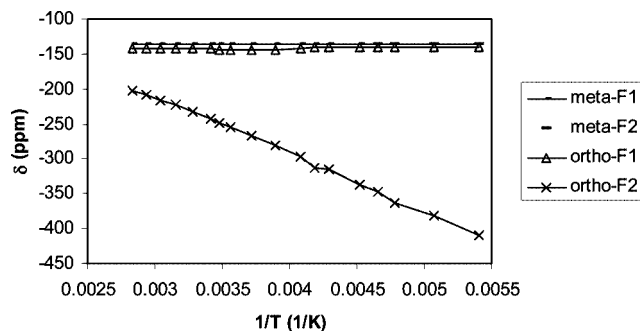


Figure 6. δ vs $1/T$ plot of the ^{19}F NMR resonances of $\text{Cp}'_2\text{Ce}'(2,3,6\text{-C}_6\text{H}_2\text{F}_3)$, **8**, in C_7D_{14} , T in Kelvin.

8, the more shielded resonance has the strongest dependence on temperature, while the less shielded resonance is weakly dependent on temperature, as are the resonances due to meta-F and para-F, Figures 5 and 6. As the temperature is lowered, each of the fluorine resonances on the meta and para sites grow another resonance. In each case the total populations are constant, and warming generates the original spectra. The ^{19}F NMR line-shape supports the contention, developed from the ^1H NMR spectra, that at least two isomers of C_s symmetry are unequally populated at low temperature and only their relative populations, but not their identities, are discernible from the line-shape behavior. The presence of isomers that differ in free energy as a result of the orientation of the substituted cyclopentadienyl rings in paramagnetic metallocenes has been postulated earlier on the basis of variable-temperature ^1H NMR spectroscopy.⁵ The fluxional NMR spectra from 20 to -50°C are consistent with a model in which the Cp' and fluorophenyl groups are dynamic. The minimum fluxional motion of the Cp' -ring is an oscillation about the pseudo- C_5 axis creating a time-

Table 2. Comparison of Averaged Bond Lengths (Å) and Angles (deg)

	Cp' ₂ CeC ₆ F ₅ ^a	Cp' ₂ Ce(2,3,4,6-C ₆ HF ₄), 6	Cp' ₂ Ce(2,3,4,5-C ₆ HF ₄), 7
Ce–C(Cp'-ring), ave	2.82 ± 0.06	2.82 ± 0.05	2.82 ± 0.06
Ce–C(Cp'-ring centroid)	2.54	2.55	2.54
Ce–C(ipso)	2.621(4)	2.623(3)	2.64 ± 0.02
Ce···F	2.682(2)	2.711(2)	2.863 ± 0.005
(Cp'-ring centroid)–Ce–(Cp'-ring centroid)	147	145	144
Ce–C(ipso)–C(ortho) ^c	97.5(3)	98.9(2)	102.6 ± 0.6
Ce–C(ipso)–C(ortho) ^d	149.7(3)	150.5(3)	140.5 ± 0.4
C(ipso)–C(ortho)–F	116.4(3)	115.2(3)	115.5 ± 0.5
Ce···F–C(ortho)	93.6(1)	93.8(2)	92.0 ± 0.7

^a From ref 1. ^b Averaged values for the two disordered molecules in the asymmetric unit, deviations are rms values. ^c The angle involved in the Ce···F interaction. ^d The angle not involved in the Ce···F interaction.

Table 3. Crystal Data

	Cp' ₂ Ce(2,3,4,6-C ₆ HF ₄), 6	Cp' ₂ Ce(2,3,4,5-C ₆ HF ₄), 7
crystal system	monoclinic	monoclinic
space group	<i>P</i> 2 ₁ / <i>n</i> , <i>Z</i> = 4	<i>P</i> 2 ₁ / <i>n</i> , <i>Z</i> = 4
<i>a</i> (Å)	10.2210(6)	10.1818(5)
<i>b</i> (Å)	22.0625(13)	22.1638(11)
<i>c</i> (Å)	18.0234(11)	17.8504(9)
β (deg)	92.369(1)	91.591(1)
<i>V</i> (Å ³)	4060.9(4)	4026.7(3)
<i>T</i> (°C)	–115	–104

averaged mirror plane rendering the top and bottom rings equivalent. The motion of the fluorophenyl ring is involved in generating another symmetry plane that results in time-averaged Me₃C groups, but this motion is not necessarily free rotation; an oscillation about the Ce–C(ipso) bond is sufficient. The limitations imposed by the paramagnetic nature of these compounds render the interpretation of their dynamic behavior qualitative.

2.3. Solid State Studies. 2.3.1. Molecular Structures of **6 and **7**.** As mentioned above, the solution ¹H NMR spectra at 20 °C of **7**, **10**, **11**, and **13** indicate that these complexes are either fluxional or they have structures that are different from **4**, **6**, **8**, **9**, **12**, and Cp'₂CeC₆F₅; the solid state structure of the latter complex is available in the literature,¹ and the X-ray crystal structures for **6** and **7** are reported below. An ORTEP diagram for **6** is shown in Figure 1, and the important bond distances and angles are listed in Table 2, along with those for **7** and Cp'₂CeC₆F₅. A partial ORTEP diagram for **7** is shown in Figure 2; the C₆HF₄-ring is disordered over two equivalent positions, but only one of the molecules is illustrated in Figure 2. Crystal data for **6** and **7** are shown in Table 3, and additional details are available as Supporting Information.

Inspection of the ORTEP diagrams and the geometrical parameters for **6** and **7**, along with these data for Cp'₂CeC₆F₅, shows that the molecular structures are similar; the Cp'-rings are staggered with identical averaged Ce–C (Cp'-ring) distances. The planar fluoroaryl rings lie essentially in a plane perpendicular to the plane defined by the (ring centroid)–Ce–(ring centroid) construction. The Ce–C(ipso) vector lies essentially on the idealized molecular C₂ axis even though one of the C(ortho)–F groups in **6** and Cp'₂CeC₆F₅ and the only C(ortho)–F group in **7** have short Ce···F contact distances. Accordingly, the Ce···F contact bends the entire C₆H_xF_(5-x), *x* = 0, 1, ring so that it does not lie on the C₂ axis.

2.3.2. Crystal Structures of **6 and **7**.** It is important that the crystal data for **7** are collected within a few days after the crystals are isolated, since the crystals of **7** change to those of **6** in the solid state, in a Schlenk tube stored inside the drybox at 20–25 °C over the time period of approximately 2 months. The single crystal used for the X-ray structure determination of **7** was obtained as shown in Scheme 3, and the crystals were obtained by crystallization from pentane. The ¹H NMR spectrum of several of these crystals dissolved in C₆D₆ showed only resonances due to **7** and pentane of crystallization. The single crystal that was used for the structure determination of **6** was obtained as shown in Scheme 2. The ¹H NMR spectrum of several of these crystals dissolved in C₆D₆ showed only resonances due to **6** and pentane.

Complexes **6** and **7** crystallize in the monoclinic crystal system in space group *P*2₁/*n* with *Z* = 4. The unit cell contains one-half of a molecule of disordered pentane in each structure. The crystal data, collected at –115 °C for **6** and –104 °C for **7**, are shown in Table 3, and the packing diagram of **6** is shown in Figure 7. The packing diagram for **7** is identical to that for **6** and is available as Supporting Information. Inspection of the packing diagrams shows that the unit cell contains considerable empty space, some of which is filled by the molecule of pentane. The closest the individual molecules approach each other is 3.03 Å.

The crystal structures of **6** and **7** are isomorphous, and the only difference is that the *a*- and *c*-dimensions of **6** are slightly longer, while the *b*-dimension is slightly shorter, relative to those of **7**, resulting in the unit cell volume of **6** being about 0.8% larger than that of **7**. The similarity in unit cell parameters precludes monitoring their change as a function of time in order to determine the rate law and rate constant for the solid state rearrangement, which means that the mechanism for the rearrangement is necessarily qualitative.

The small change in unit cell parameters shows that the rearrangement of **7** to **6** is not driven by a favorable change in the free energy of the ensemble, but the rearrangement is driven by a favorable change in ΔG of the individual molecules in the ensemble, that is, molecules of **6** have lower free energy than those of **7**. The ensemble, however, plays a critical role since it allows **7** to rearrange cleanly to **6** without formation of detectable amounts of Cp'₂CeF and a benzyne, a pathway that both complexes follow in the solution at 20 °C, over a much shorter time period. This behavior implies that the rearrangement mechanism in the solid state does not proceed by formation of Cp'₂CeF and a “free” benzyne followed by trapping of the benzyne by Cp'₂CeF, i.e., a reversible stepwise process. The solid state environment either prevents benzyne from escaping and ensures that the benzyne is trapped by Cp'₂CeF, or the “free”

(5) (a) Lukens, W. W.; Beshouri, S. M.; Stuart, A. L.; Andersen, R. A. *Organometallics* **1999**, *18*, 1247–1252. (b) Zi, G.; Blosch, L. L.; Jia, L.; Andersen, R. A. *Organometallics* **2005**, *24*, 4602–4612.

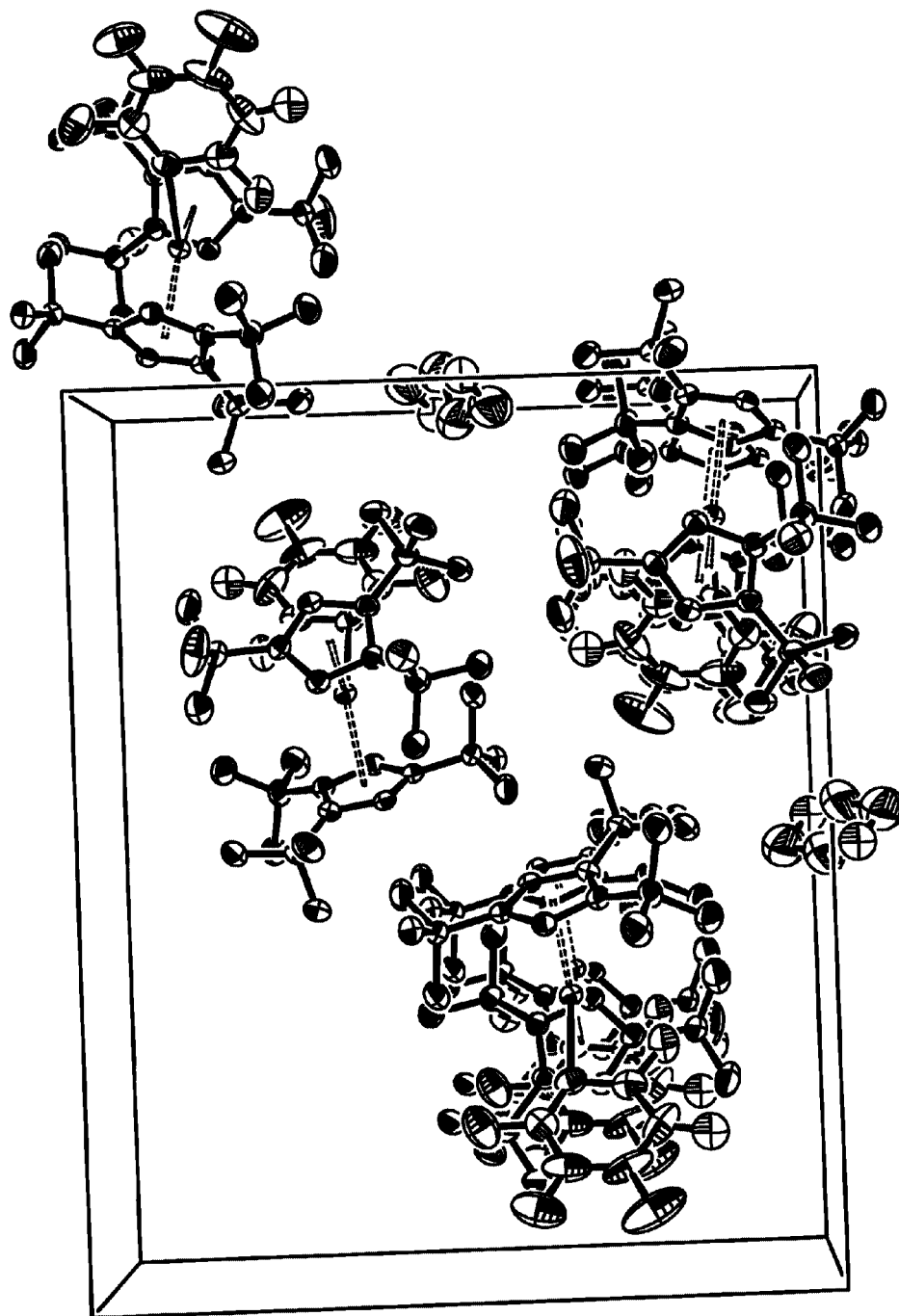


Figure 7. Crystal packing diagram for $\text{Cp}'_2\text{Ce}(2,3,4,6\text{-C}_6\text{HF}_4)$, **6**.

benzyne never forms, implying that the mechanism of the $\text{Cp}'_2\text{Ce}$ and F site exchange between C(35) and C(36) is synchronous. Although the rearrangement mechanism can only be described qualitatively, the rearrangement proceeds quantitatively and irreversibly in the solid state, and the net reaction is exoergic.

3. Discussion

The reaction products that form when $\text{Cp}'_2\text{CeH}$ is exposed to a series of hydrofluorobenzenes, $\text{C}_6\text{H}_{6-x}\text{F}_x$, $x = 2 - 5$, are shown in Schemes 1–9 and summarized in Chart 2. The only product, or the major product, that forms when $x = 2, 3, 4$, or

5, with two exceptions, always shows a regiochemistry in which both of the ortho sites in the fluoroaryl ligand in $\text{Cp}'_2\text{Ce}-\text{C}_6\text{H}_{5-x}\text{F}_x$ are occupied by fluorine atoms, symbolized as $\text{Ce}-\text{C}_i\text{C}_o(\text{F},\text{F})$. The only exceptions to this generalization are the reactions between $\text{Cp}'_2\text{CeH}$ and 1,4-difluorobenzene or 1,2-difluorobenzene, which can only afford isomers in which one ortho site is occupied by a fluorine atom, viz., $\text{Ce}-\text{C}_i\text{C}_o(\text{F},\text{H})$. This general substitution pattern presumably reflects the trend in CeC bond dissociation enthalpies (bond strengths) which then lie in the order $\text{Ce}-\text{C}_i\text{C}_o(\text{F},\text{F}) > \text{Ce}-\text{C}_i\text{C}_o(\text{F},\text{H}) > \text{Ce}-\text{C}_i\text{C}_o(\text{H},\text{H})$. Unfortunately, these experimental bond dissociation enthalpies are not known, but the solid state rearrangement of **7** to **6** clearly shows that the inequality is $\Delta H \text{Ce}-\text{C}_i\text{C}_o(\text{F},\text{F}) >$

Chart 2. Fluoroarene Reaction Products with Cp₂CeH

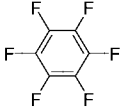
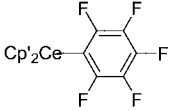
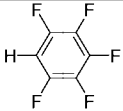
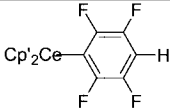
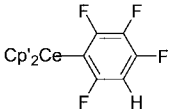
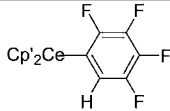
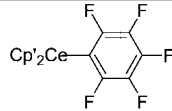
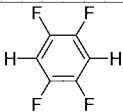
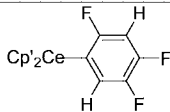
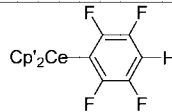
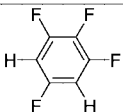
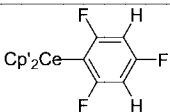
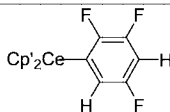
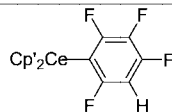
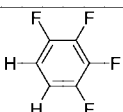
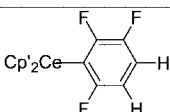
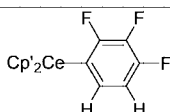
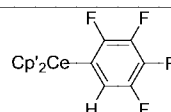
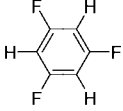
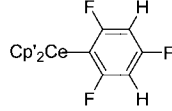
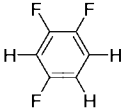
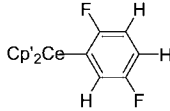
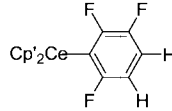
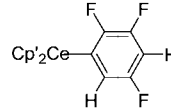
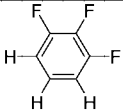
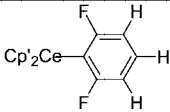
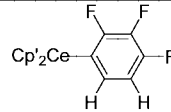
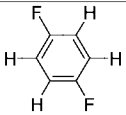
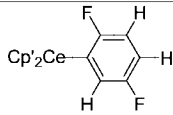
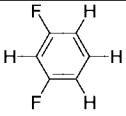
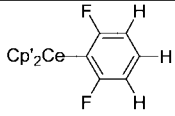
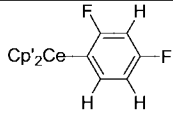
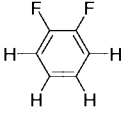
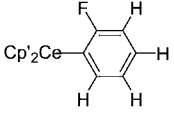
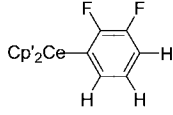
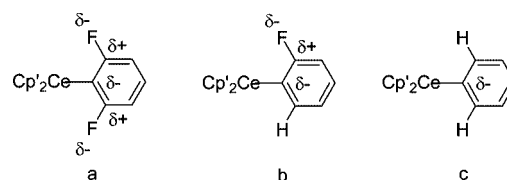
polyfluorobenzene	Possible products			
	CF activation		CH activation	
	C ₁ C ₀ (F,F)	C ₁ C ₀ (F,H)	C ₁ C ₀ (F,F)	C ₁ C ₀ (F,H)
	 major			
	 minor  not observed	 not observed	 major	
		 not observed	 major	
	 not observed	 not observed	 major	
	 major	 not observed		 minor
			 major	
		 not observed	 major	 not observed
	 major			 not observed

Chart 2. Continued

polyfluorobenzene	Possible products			
	CF activation		CH activation	
	$C_iC_o(F,F)$	$C_iC_o(F,H)$	$C_iC_o(F,F)$	$C_iC_o(F,H)$
			 major	
			 major	 not observed
		 not observed		 major

ΔH $Ce-C_iC_o(F,H)$, since the change in translational entropy is zero, and therefore $\Delta H \approx \Delta G$, assuming that the Ce-substituted cyclopentadienyl bond enthalpy is constant. Support for this inequality is derived from experimental and calculational bond dissociation enthalpies in $CpRe(CO)_2C_6H_{5-x}F_x$.⁶ The experimental values of the $Re-C(C_6H_{5-x}F_x)$ bond dissociation enthalpies (where known) agree with the calculated ones, which lie in the order $Re-C_iC_o(F,F) > Re-C_iC_o(F,H) > Re-C_iC_o(H,H)$. The origin of this order parallels the increase in electrostatic contribution to the net bond dissociation enthalpy, while the orbital contribution remains essentially constant. This postulate is supported by the calculated charge on C_i from a natural population analysis (NPA), which shows that the charge density on C_i increases in the order $C_iC_o(F,F) > C_iC_o(F,H) > C_iC_o(H,H)$. Thus, two fluorine atoms located in the ortho sites of a fluoro-substituted aryl group increase the negative charge on the ipso site more than does one fluorine atom, which in turn is higher than when both of the ortho sites contain hydrogen atoms.

This model should be applicable to the Ce–C bond dissociation enthalpies for the compounds mentioned above, since lanthanide–X bond dissociation enthalpies are dominated by electrostatic contributions, i.e., they are dominated by the Coulombic attraction between the two charges $M(+)-X(-)$.⁷ Extending this model to the compounds described in this article yields the charge distribution at C(ipso) and C(ortho) shown in Chart 3. The electronegative fluorine atom will induce a larger positive charge on the carbon atom to which it is bonded than will the less electronegative hydrogen atom, which in turn

Chart 3. Charge Distribution in $Cp'_2CeC_6H_{5-x}F_x$ 

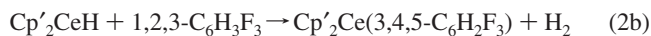
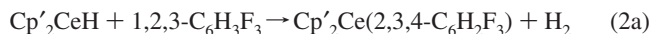
induces a larger negative charge on the ipso-carbon atom. This thermodynamic model is in accord with the product formed in the reaction between Cp'_2CeH and the hydrofluorobenzenes in Chart 2 and the solid state rearrangement of **7** to **6**. Although the translational entropy for the solid state rearrangement of **7** to **6** is zero, the entropy content in **6** is greater than that in **7**, since two $Ce(ortho)-F$ interactions are available in **6** but only one in **7**. Thus, the vibrational entropy in the two complexes is not identical, and the rearrangement is favored enthalpically and entropically.⁸

Although the thermodynamics of the rearrangement is clear the mechanism is not. In the initial paper, the calculated mechanism of the reactions of Cp'_2CeH (modeled by Cp_2LaH) with either C_6F_6 or C_6HF_5 proceed by way of σ -bond metathesis transition states in which the barrier for the CeH for CH exchange process is about 20 kcal mol^{-1} lower than that for CeH for CF exchange, resulting in the generalization that CF activation products are not observed when CH bonds are present in the hydrofluorobenzene.¹ Extension of this generalization leads to a conflict with the products formed in the reaction of Cp'_2CeH with 1,2,3,4-tetrafluorobenzene and 1,2,3-trifluorobenzene. In both of these reactions, the products derived from CeH for CF and CH activation are observed; the major product in both reactions is derived from CF activation. If the CH activation step occurs with a barrier lower than that of the CF activation step, the products of the reaction of Cp'_2CeH and 1,2,3-trifluorobenzene would be those shown in eqs 2a and 2b.

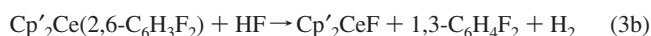
(6) (a) Carbo, J. J.; Eisenstein, O.; Higgitt, C. L.; Klahn, A. H.; Maseras, F.; Oelckers, B.; Perutz, R. N. *J. Chem. Soc., Dalton Trans.* **2001**, 9, 1452–1461. (b) Clot, E.; Besora, M.; Maseras, F.; Megret, C.; Eisenstein, O.; Oelckers, B.; Perutz, R. N. *Chem. Commun.* **2003**, 4, 490–491.

(7) (a) Johnson, D. A. *Some Thermodynamic Aspects of Inorganic Chemistry*, 2nd ed.; Cambridge University Press: Cambridge, 1982; Chapters 2 and 6. (b) Pankratz, L. B. *Thermodynamic Properties of Halides*, Bulletin 674; U.S. Bureau of Mines, 1984. (c) Nolan, S. P.; Hedden, D.; Marks, T. J. *Bonding Energetics in Organolanthanide Chemistry*; Marks, T. J. Ed.; ACS Symposium Series 428; American Chemical Society: Washington, DC, 1990; p 159.

(8) We thank a reviewer for calling our attention to the fact that the vibrational entropy of **6** is greater than that of **7**.



Although the C–H isomer illustrated in 2a, **10**, is formed, the major product is the result of CF activation, Cp'₂Ce(2,6-C₆H₃F₂), **12**, Schemes 6 and 8. A set of elementary reactions that account for the formation of **12** are those illustrated in eqs 3a–c. If true, **12** is formed by two pathways, 3a and 3c; 3a is a CeH/CF exchange while 3c is a CeH/CH exchange. The H/F interchange reaction, 3b, is likely to occur with a low activation barrier;¹ this process along with the reaction symbolized by 3a yields Cp'₂CeF. Reaction 3c demands that Cp'₂CeH is not depleted in reactions 3a and 3b, which means that the barrier for the reaction 3c must be comparable with that of 3a.



A similar contradiction is apparent in the reaction of 1,2,3,4-tetrafluorobenzene in which the major product is **8**, Scheme 3, the result of Ce–H/CF exchange. Indeed, the contradiction also extends to C₆F₆ and C₆HF₅.¹ The contradiction between the calculational and experimental studies described in this article may be rationalized in the following ways: (a) the calculational methodology does not correctly deal with the large amount of charge reorganization in the transition state in the CeH for CF exchange, (b) the mechanism of reaction may not proceed by way of a σ-bond metathesis mechanism, or (c) the bulky substituted cyclopentadienyl ligands influence the barriers more than expected, since unsubstituted cyclopentadienyl ligands are used in the calculations.

4. Conclusions

The stereochemical principle that emerges from the experimental studies described in this article is that when a choice of regioisomers is available, the isomer that is observed exclusively or in the highest yield is always the one in which the fluoroaryl group contains fluorine atoms in both of the ortho sites of the polyfluorophenyl derivative. This thermodynamic result is postulated to be dictated by the CeC bond dissociation enthalpy that is controlled by the electronegative fluorine atoms that induce polarization at the ortho-carbon atoms, C_o(δ⁺)–F(δ[–]), which in turn induces a negative charge on the ipso-carbon, Ce–C_i(δ[–]). Thus the strongest Ce–C_i is formed when both ortho carbons of the phenyl ring contain fluorine substituents. The elementary reactions that comprise the net reaction are consistent with the postulate that the activation energy for CH and CF have comparable values, and the stereochemistry of the product is determined by the change in free energy of the net reaction rather than the activation energy of the elementary reactions. The thermodynamic control is dramatically illustrated by the irreversible solid state rearrangement (25 °C) of **7** to **6**, a CeC(ipso) for C(ortho)F site exchange.

5. Experimental Details

5.1. General. All manipulations were performed under an inert atmosphere using standard Schenk and dry box techniques. All solvents were dried and distilled from sodium or sodium benzophenone ketyl. Fluoro and hydrofluorobenzenes, obtained from Aldrich Chemical Co., were dried and vacuum transferred from calcium hydride; the isomer purity was assayed by ¹H and ¹⁹F NMR

spectroscopy. NMR spectra were recorded on Bruker AV-300 or AV-400 spectrometers at 20 °C in the solvent specified. ¹⁹F NMR chemical shifts are referenced to CFCl₃ at 0 ppm. J-Young NMR tubes were used for all NMR tube experiments. Electron impact mass spectrometry and elemental analyses were performed by the microanalytical facility at the University of California, Berkeley. The abbreviation Cp' is used for the 1,2,4-tri-*tert*-butylcyclopentadienyl ligand.

5.2. General Procedure for NMR Tube Reactions of C₆H_{6-x}F_x with Cp'₂CeH, **1.** Cp'₂CeH¹ was dissolved in C₆D₆ or C₆D₁₂ in an NMR tube, and a drop of the desired fluorobenzene was added. The solution turned from purple to orange, and gas bubbles were evolved. The sample was analyzed by ¹H and ¹⁹F NMR spectroscopy. Decomposition over time was observed by NMR spectroscopy, first at 20–25 °C over 3–7 days and then at 60 °C for one day. Products are summarized in Chart 2 and ¹H and ¹⁹F NMR resonances are listed in Table 1. Samples for GC/MS were prepared by adding a drop of H₂O, agitating, and allowing the samples to stand closed for 10 min. The samples were then dried over magnesium sulfate, filtered, and diluted 10-fold with pentane. A 1 μL sample was injected into a HP6890 GC system with a J&W DB-XLB universal nonpolar column, attached to an HP5973 Mass Selective Detector. The principle elution peaks consisted of free Cp'H and the cycloaddition product(s) of the fluorobenzene(s) and benzene or Cp'H.

5.3. General Procedure for NMR Tube Reactions of C₆H_{6-x}F_x with the Metallacycle Cp'[(Me₃C)₂C₅H₂C(Me₂)CH₂]Ce, **2.** Cp'₂CeCH₂C₆H₅¹ was dissolved in C₆D₁₂ in an NMR tube and heated at 60 °C for one day, which yielded the metallacycle. A drop of the desired fluorobenzene was added, and the solution turned from purple to orange. Subsequent handling and analysis were identical to those for reactions with Cp'₂CeH. The synthetic details for two specific reactions that yielded isolated compounds are described below.

5.4. Cp'₂Ce(2,3,4,5-C₆HF₄), **7.** Cp'₂CeCH₂C₆H₅ (0.5 g, 0.7 mmol) was dissolved in pentane (10 mL) and stirred at room temperature for 48 h, producing a solution of Cp'[(Me₃C)₂C₅H₂–C(Me₂)CH₂]Ce. 1,2,3,4-Tetrafluorobenzene (0.18 mL, 1.7 mmol) was added via syringe. The purple solution turned orange over 20 min. The solution volume was reduced to 5 mL, and the solution was cooled to –10 °C, yielding orange crystals. Yield: 0.2 g (0.26 mmol), 37%. The low yield was due to the high solubility of the compound. ¹H NMR (C₆D₁₂) δ –1.90 (36H, ν_{1/2} = 120 Hz), –9.59 (18H, ν_{1/2} = 80 Hz), ¹⁹F NMR (C₆D₁₂) δ –137.0 (1F, d, J = 18 Hz), –161.8 (1F, d, J = 18 Hz), –161.6 (1F, dd, J = 18, 18 Hz). The solid material decomposed rapidly above 135 °C, which precluded analysis by EI-MS. Full crystallographic details are included as Supporting Information: Monoclinic cell space group, P2₁/n: a = 10.1818(5) Å, b = 22.164(1) Å, c = 17.8504(9) Å, β = 91.591(1)°, V = 4026.7(3) Å³.

5.5. Cp'₂Ce(2,3,4,6-C₆HF₄), **6.** Cp'₂Ce(2,3,4,5-C₆HF₄) (0.2 g, 0.26 mmol) was allowed to stand at 25 °C for 2 months. A sample was dissolved in C₆D₁₂ and analyzed by ¹H and ¹⁹F NMR spectroscopy, which indicated quantitative conversion to Cp'₂Ce(2,3,4,6-C₆HF₄). Yield: 0.2 g (0.26 mmol), 100%. This complex was also prepared from the metallacycle and 1,2,3,5-tetrafluorobenzene in a procedure analogous to that described above. ¹H NMR (C₆D₁₂) δ 0.17 (1H, d, J = 7 Hz), –1.44 (18H, ν_{1/2} = 100 Hz), –2.09 (18H, ν_{1/2} = 90 Hz), –9.58 (18H, ν_{1/2} = 70 Hz), ¹⁹F NMR (C₆D₁₂) δ –139 (1F, dd, J = 18, 7 Hz), –151 (1F, ν_{1/2} = 200 Hz), –166 (1F, d, J = 15 Hz), –242 (1F, ν_{1/2} = 200 Hz). The solid material decomposed rapidly above 135 °C, which precluded analysis by EI-MS. Full crystallographic details are included as Supporting Information: Monoclinic cell space group, P2₁/n: a = 10.2210(6) Å, b = 22.063(1) Å, c = 18.024(1) Å, β = 92.369(1)°, V = 4060.9(4) Å³.

Crystallographic data for the structures in this paper have been deposited with the Cambridge Crystallographic Data Centre. Copies of the data (CCDC 671970 and 671971) can be obtained free of

charge via www.ccdc.cam.ac.uk/data_request/cif, by emailing data_request@ccdc.cam.ac.uk, or by contacting The Cambridge Crystallographic Data Centre, 12, Union Road, Cambridge CB2 1EZ, U.K.; fax +44 1223 336033. Structure factor tables are available from the authors.

Acknowledgment. This work was partially supported by the Director of Energy Research Office of Basic Energy Sciences, Chemical Sciences Division of the U.S. Department of Energy under Contract No DE-AC02-05CH11234. We thank Dr. Fred Hollander and Dr. Allen Oliver for their assistance with the crystallography

(at CHEXRAY the U.C. Berkeley X-ray diffraction facility), and Odile Eisenstein and Laurant Maron for discussions and comments.

Supporting Information Available: Labeling diagrams, tables giving atomic positions and anisotropic thermal parameters, bond distances and angles, and least-squares planes for each structure. This material is available free of charge via the Internet at <http://pubs.acs.org>.

JA800639F